Intra- and Intermolecular Steric Hindrance Effects Induced Higher Open-Circuit Voltage and Power Conversion Efficiency

Liangliang Han,[†] Weichao Chen,[†] Tong Hu,[‡] Junzhen Ren,[‡] Meng Qiu,[†] Yuanhang Zhou,[†] Dangqiang Zhu,[†] Ning Wang,[†] Mingliang Sun,[‡] and Renqiang Yang*,[†,§]

[†]CAS Key Laboratory of Bio-based Materials, Qingdao Institute of Bioenergy and Bioprocess Technology, Chinese Academy of Sciences, Qingdao 266101, China

[‡]Institute of Material Science and Engineering, Ocean University of China, Qingdao 266100, China

[§]State Key Laboratory of Luminescent Materials and Devices, South China University of Technology, Guangzhou 510641, China

S *Supporting Information*
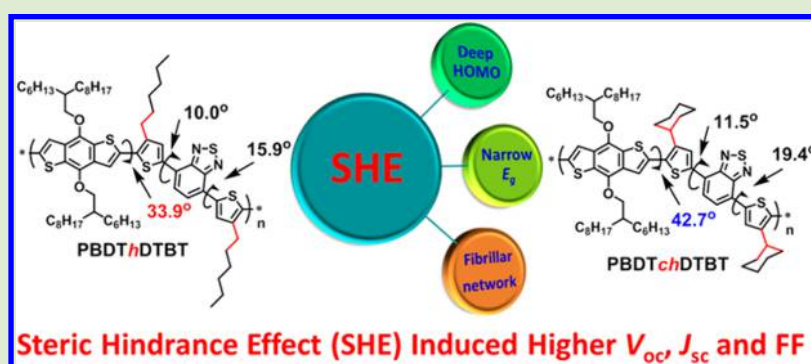
ABSTRACT: A pair of donor−acceptor polymers PBDT*h*DTBT and PBDT*ch*DTBT are synthesized, which share the same conjugated backbone, but are designed with hexyl and cyclohexyl side chains, respectively. The stronger steric hindrance of cyclohexyl endows PBDT*ch*DTBT a deeper lying HOMO energy level of −5.39 eV compared to −5.22 eV for PBDT*h*DTBT. However, PBDT*h*DTBT and PBDT*ch*DTBT exhibit a similar optical bandgap around 1.72 eV and a hole mobility around 10^{-5} $cm^2\,V^{-1}\,s^{-1}$. Interestingly, the PBDT*ch*DTBT/PC$_{71}$BM blends exhibited higher hole mobility than PBDT*h*DTBT/PC$_{71}$BM after DIO was added. The higher hole mobility and fibrillar network in the active layer endows PBDT*ch*DTBT higher power conversion efficiency of 7.9%, together with simultaneously improved open-circuit voltage of 0.80 V, short-circuit current density of 13.50 mA cm^{-2}, and fill factor of 72.74% after a systemic study of their solar cell devices.

Semiconducting polymer is considered as the ideal material for next generation large area optoelectronics application in virtue of its superior solution processing and film forming ability.[1−5] When a semiconducting polymer is employed, research is mainly focused on its frontier molecular orbital energy levels and optical and optoelectronic characteristics, which have reliance on the polymer's planarity, interchain aggregation, alkyl substituents, and molecular weight.[6−9] One simple and effective strategy employed to adjust the energy levels and optical property of a semiconducting polymer is intra- or intermolecular steric hindrance effect (SHE).[10−13] However, SHE has been reported with negative effect on molecular self-organization in the donor−acceptor (D−A) oligmers.[14] Intermolecular SHE introduced to the polymer backbone could prevent molecular packing and then result in weaker crystallinity.[15] Intramolecular SHE may reduce the π-orbital overlap between two adjacent units and lead to undesirable hypochromatic shifted absorption spectra and wide bandgap (E_g),[10,16−20] however, as is well-known, wide

absorption spectra, and narrow E_g of the absorber are crucial for organic solar cells (OSCs) application.[21]

Although SHE has been considered as a negative effect for polymer's self-aggregation and effective conjugation, one advantage should be pointed out, that is, SHE can significantly decrease the highest occupied molecular orbital (HOMO) energy levels of the polymer. For example, poly(3-cyclo-hexylthiophene) (P3*ch*T) exhibited more twisted conjugating backbone than poly(3-hexylthiophene) (P3*h*T) because of stronger SHE of cyclohexyl than hexyl, which resulted in a larger dihedral angle (θ) between the two adjacent thiophene rings together with a wider E_g and a deeper lying HOMO of −5.72 eV, 0.72 eV lower than that of P3*h*T (−5.0 eV) experimentally.[10] Theoretically, Brédas and co-workers reported that the ionic potential of the polythiophene increased gradually as the torsion angle increased from 0 to 90°.[22] This

will be very interesting for OSCs application, which is composed of a polymeric donor and a fullerene acceptor, and the deeper lying HOMO of the polymer donor will be beneficial for higher open-circuit voltage (V_{oc}).[23] Several examples have been reported employing SHE (alkyl side chains) to design deeper HOMO polythiophenes with improved V_{oc} in their OSCs, unfortunately, E_g of the polymers became wider together with decreased hole mobility (μ_{hole}), which resulted in lower short-circuit current density (J_{sc}), fill factor (FF), and inconspicuous improvement of power conversion efficiency (PCE) compared to P3hT.[24] Further-more, lower J_{sc}, FF, and extremely low μ_{hole} were also obtained when SHE was employed to design an indacenodithiophene-based polymer for OSCs application.[25] Thus, it can be seen, employing simple SHE to design semiconducting polymer for highly efficient OSCs will be a challenging issue. A comprehensive survey of the chemical methods for designing high PCE polymers found that the inductive effect such as introducing fluorine or sulfur atoms to the polymer backbone has been considered as one of the most effective and successful methods, which can bring about simultaneous improvement of V_{oc}, J_{sc}, and FF on their OSCs devices.[26−30] However, chemically introducing fluorine[31] or sulfur[32] always makes the synthetic route more complicated and expensive, and fluorine atoms sometimes reduce the solubility of the polymers remarkably.[33]

In this communication, we reported two D−A polymers incorporating 4,8-bis(hexyldecyloxy)benzo[1,2-b:4,5-b']-dithiophene (alkoxy−BDT) as the donor unit and either 4,7-bis(4-hexylthiophen-2-yl)benzo[c][1,2,5]thiadiazole (hDTBT) or 4,7-bis(4-cyclohexylthiophen-2-yl)benzo[c][1,2,5]-thiadiazole (chDTBT) as the acceptor unit (Scheme 1). As

Scheme 1. Synthesis of PBDThDTBT and PBDTchDTBT
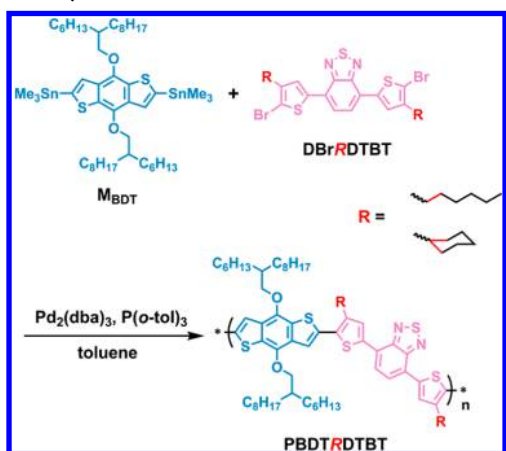
shown in Scheme 1, analogous hexyl and cyclohexyl were chosen as side chains because they have the same carbon number and similar electronic effect except they were connected to the polymer backbone with a primary carbon and a secondary carbon, respectively. PBDTchDTBT exhibited a deeper lying HOMO of −5.39 eV compared to −5.22 eV for PBDThDTBT. Interestingly, the two polymers had almost the same E_g. In their OSC devices, PBDTchDTBT exhibited higher V_{oc}, J_{sc}, and FF than PBDThDTBT, giving rise to a PCE value up to 7.9%, which was much higher than that of PBDThDTBT (5.9%). These obvious improvements were ascribed to a deeper lying HOMO of PBDTchDTBT together with a tunable fine

nanoscale fibrillar network in PBDTchDTBT/[6,6]-phenyl C$_{71}$ butyric acid methyl-ester (PC$_{71}$BM) blend. To our knowledge now, SHE is first designed with simultaneously improved V_{oc}, J_{sc}, and FF for OSCs application, and 7.9% is the highest PCE among alkoxy-BDT and DTBT copolymers.[34]

4,7-Bis(5-bromo-4-hexylthiophen-2-yl)benzo[c][1,2,5]-thiadiazole (DBrhDTBT)[35] and 2,6-bis(trimethyltin)-4,8-bis-(hexyldecyloxy)benzo[1,2-b:4,5-b']dithiophene (M$_{BDT}$)[36] were synthesized according to the literature methods. The cyclohexyl substituted monomer 4,7-bis(5-bromo-4-cyclohexylthiophen-2-yl)benzo[c][1,2,5]thiadiazole (DBrchDTBT) was first reported here with similar synthetic route of DBrhDTBT (Scheme S1). The final copolymers PBDThDTBT and PBDTchDTBT were prepared via Stille coupling polymerization. PBDThDTBT and PBDTchDTBT show excellent solubility in halogenated solvents and high number-average molecular weight (M_n) of 57.2 kg mol^{-1} and 38.8 kg mol^{-1} with polydispersity index (PDI) of 2.4 and 2.0, respectively. The relative lower M_n of PBDTchDTBT compared to PBDThDTBT may be because of the stronger SHE of cyclohexyl than hexyl, which made the Stille coupling copolymerization more difficult. However, the relatively high molecular weights of PBDThDTBT and PBDTchDTBT indicated an efficient polymerization reaction occurred. PBDThDTBT and PBDTchDTBT exhibited nearly indistinguishable decomposition temperature (T_d) with 5% weight loss denoted at ∼318 °C (Figure S1).

The onset oxidation potential of PBDThDTBT was estimated at about 0.82 V (Figure S2), and the HOMO was calculated to be −5.22 eV relative to ferrocene as an internal standard. Interestingly, because of the SHE of cyclohexyl side chain, PBDTchDTBT exhibited a higher oxidation potential with an onset at 0.99 V, a deeper HOMO of −5.39 eV was derived. The dihedral angles in the repeated BDThDTBT and BDTchDTBT units were optimized with the density functional theory (DFT) method under B3LYP/6-31G(d,p) level.[37] As shown in Figure S3, PBDTchDTBT exhibited a larger $\theta 1 = 42.7°$ compared to $\theta 1 = 33.9°$ of PBDThDTBT. The larger $\theta 1$ of PBDTchDTBT showed us clearly stronger intramolecular SHE of cyclohexyl than hexyl which could reduce the π-orbital overlap between BDT and adjacent thiophene rings and result in a deeper lying HOMO.

In dilute solutions, as shown in Figure 1, PBDThDTBT and PBDTchDTBT exhibited almost unanimous intramolecular CT transition absorption[38] centered at ∼595 nm, indicating that although cyclohexyl could result in larger $\theta 1$, however, such
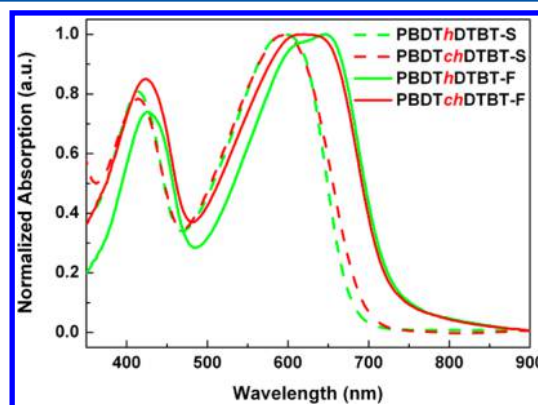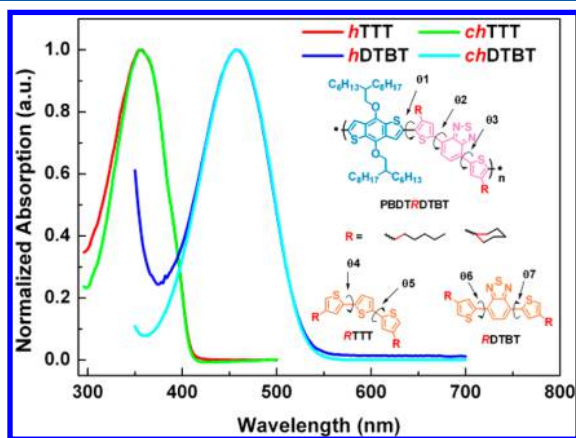

Figure 1. UV−vis absorption spectra of PBDThDTBT and PBDTchDTBT in chloroform solutions (S) and neat films (F).

intramolecular SHE can negligibly affect the CT transition state. In their solid state films, PBDT*ch*DTBT exhibited slightly blue-shifted peak wavelength (λ_{max} = 616 nm). The reason may be that cyclohexyl reduced the intermolecular aggregation of the polymer because of its stronger intermolecular SHE. However, there was nearly no change of the absorption edge (λ_{edge}) for PBDT*ch*DTBT compared to PBDT*h*DTBT, and, interestingly, PBDT*ch*DTBT exhibited wider absorption spectra with full width at half maximum estimated to be 170 nm in the CT transition band, 10 nm wider than that of PBDT*h*DTBT. The optical E_g of PBDT*h*DTBT and PBDT*ch*DTBT were estimated to be 1.71 and 1.72 eV, respectively, indicating efficient CT transition states and interchain aggregation existed in both the polymers although sterically hindered cyclohexyl was introduced in PBDT*ch*DTBT. The lowest unoccupied molecular orbitals (LUMOs) of PBDT*h*DTBT and PBDT*ch*DTBT were calculated as −3.51 and −3.67 eV, respectively. Both the HOMO and LUMO of PBDT*ch*DTBT down-shifted, while the E_g of the two polymers were almost identical. However, the cyclohexyl will destroy the π−π conjugation for P3*ch*T by reducing the π orbital overlap along the whole backbone and resulting in wider E_g.[10]

Both the polymers have three dihedral angles per repeat unit as depicted in Figure 2 and simulated in Figure S3. Obviously,
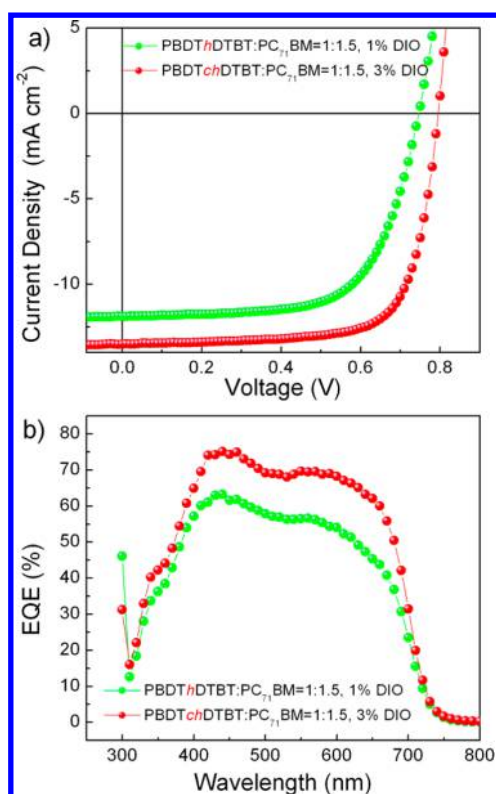

Figure 2. UV−vis absorption spectra of *R*TTT and *R*DTBT in hexane solutions (Inset: molecular structures and dihedral angles existed in the D−A polymers PBDT*R*DTBT, π−π conjugating oligmers *R*TTT, D−A type molecules *R*DTBT).

larger $\theta 1$ can significantly influence the effective conjugation between BDT and thiophenes and resulted in a deeper lying HOMO. However, the wide absorption of these D−A polymers was originated from the CT transition state between the electron donating group and electron withdrawing unit. Here, benzo[*c*][1,2,5]thiadiazole (BT) unit plays the role of electron acceptor; therefore, effective conjugation is indispensable between BT and flanking thiophene rings. $\theta 2$ and $\theta 3$ usually determine whether effective conjugation and CT transition states exist in the DTBT system.[39] In order to elucidate how the substituents could affect $\theta 2$ and $\theta 3$ in the D−A polymers, we designed two π−π conjugating small molecules 2,5-bis(4′-hexyl-2′-thienyl)thiophene (*h*TTT) and 2,5-bis(4′-cyclohexyl-2′-thienyl)thiophene (*ch*TTT); in addition, D−A-type oligomers *h*DTBT and *ch*DTBT were also included (Figure 2, inset). In the oligomer thiophene systems, their absorption originated from the π−π conjugation was very sensitive to the twisted

angle of the adjacent thiophenes.[40] Two dihedral angles $\theta 4$ and $\theta 5$ existed in *h*TTT or *ch*TTT, and their absorption spectra (Figure 2, hexane solutions) were almost identical with the same λ_{max} = 355 nm and λ_{edge} = 410 nm, which indicated effective π-orbital overlap between adjacent thiophene rings both in *h*TTT and *ch*TTT, and the 4-position substituents can hardly influence $\theta 4$ and $\theta 5$. In the D−A system, same phenomena were observed, and efficient CT transition between thiophene and BT occurred regardless of the 4-positions were substituted with hexyl or sterically hindered cyclohexyl. From which we infer PBDT*h*DTBT and PBDT*ch*DTBT possess similar $\theta 2$ and $\theta 3$, respectively, which warrants effective CT transition in both the polymers. The simulated results also show us a little differences between the two dihedral angles ($\Delta \theta 2$ = 1.5° and $\Delta \theta 3$ = 3.5°, Figure S3). This can help to explain why PBDT*h*DTBT and PBDT*ch*DTBT exhibited similar CT transition absorption in their dilute solutions. And the slightly blue-shifted λ_{max} for PBDT*ch*DTBT in the film state was the result of intermolecular SHE of cyclohexyl and such steric hindrance showed negligible effects of the polymer E_g. It should be pointed out that the electrochemical and optical differences of PBDT*ch*DTBT compared to PBDT*h*DTBT were mainly induced by SHE because the electronic effects of nonchromophoric cyclohexyl and hexyl can be eliminated compared to some conjugated side chains.[41] This will be an encouraging strategy to design D−A polymers in conformity with the "weak donor−strong acceptor" ideology.[42]

Solar cells were fabricated with a conventional device structure ITO/PEDOT:PSS/polymer:PC$_{71}$BM/Ca/Al and measured under the illumination of AM 1.5 G (100 mW cm^{-2}).[43] Initially, different donor/acceptor ratios (1:1, 1:1.5, 1:2, and 1:2.5) were examined to find the optimum weight ratio (Figure S4). At a ratio of 1:1, a high V_{oc} of 0.84 V was obtained for PBDT*ch*DTBT and 0.07 V higher than that of PBDT*h*DTBT, which was even higher than the alkoxy-BDT and fluorinated DTBT incorporated polymer.[44] As PC$_{71}$BM amount increased, all the devices of PBDT*ch*DTBT exhibited higher V_{oc} than PBDT*h*DTBT at specific polymer/PC$_{71}$BM ratios (Table S1 and Figure S5). 1,8-Diiodooctane (DIO) was used as the additive to optimize the morphology of the polymer/PC$_{71}$BM blends.[45,46] In the PBDT*h*DTBT/PC$_{71}$BM blend, DIO was added with volume fraction of 1, 1.5, and 2%, unfortunately, the PCE declined gradually as the DIO volume fraction increased (Figure S6 and Table S2). For PBDT*ch*DTBT/PC$_{71}$BM blend, when 1% DIO was added, the J_{sc} was improved significantly to 12.27 mA cm^{-2}, which resulted in a higher PCE of 6.6%. When 3% DIO was added, a higher J_{sc} of 13.50 mA cm^{-2} was obtained and the FF improved to 72.74%, highly efficient OSCs with PCE = 7.9% was realized (Figure 3a and Table 1). The EQE spectra of PBDT*ch*DTBT was higher than PBDT*h*DTBT in the whole response wavelength from 300−750 nm, as shown in Figure 3b, resulting in higher J_{sc} of the device based on PBDT*ch*DTBT than PBDT*h*DTBT. The J_{sc} values (10.55 mA cm^{-2} for PBDT*h*DTBT and 13.48 mA cm^{-2} for PBDT*ch*DTBT) calculated from the integration of the EQE spectra agreed well with the J_{sc} values recorded from the J−V measurements.

The only difference of PBDT*h*DTBT and PBDT*ch*DTBT structurally was the nonchromophoric alkyl chains, besides which, both the polymers shared the same conjugating backbone together with comparative E_g and μ_{hole} of 1.23 × 10^{-5} cm^2 V^{-1} s^{-1} and 1.07 × 10^{-5} cm^2 V^{-1} s^{-1}, respectively, measured using space−charge−limited−current (SCLC) model

Figure 3. J–V (a) and EQE (b) curves of the devices based on PBDThDTBT and PBDTchDTBT.

Figure 4. AFM height (2×2 μm, a-1, b-1, c-1, d-1), phase (a-2, b-2, c-2, d-2), and TEM (a-3, b-3, c-3, d-3) images of the active layers containing PBDThDTBT/PC$_{71}$BM (a), PBDThDTBT/PC$_{71}$BM with 1% DIO (b), PBDTchDTBT/PC$_{71}$BM (c), and PBDTchDTBT/PC$_{71}$BM with 3% DIO (d).

Table 1. Device Parameters of PBDThDTBT/PC$_{71}$BM = 1:1.5 with 1% DIO and PBDTchDTBT/PC$_{71}$BM = 1:1.5 with 3% DIO (h: PBDThDTBT; ch: PBDTchDTBT)

entry	V_{oc} (V)	J_{sc} (mA cm^{-2})	FF (%)	PCE[a] (%)
h	0.75	11.60	68.22	5.9 (5.8)
ch	0.80	13.50	72.74	7.9 (7.7)

[a]Average PCE in brackets (10 devices).

(Figure S7). In order to better explain their different photovoltaic properties, atom force microscopy (AFM), and bright field transmission electron microscopy (TEM) were used to explore their morphology and phase separation characteristics. Both PBDThDTBT and PBDTchDTBT exhibited good film-forming ability with root-mean-square (RMS) surface roughness <3 nm in their neat films (Figure S8). Smooth films can also be observed from the AFM height images of polymer/PC$_{71}$BM blends, as shown in Figure 4a-1,b-1,c-1,d-1. However, serious phase separation can be observed from the phase images given from AFM phase (Figure 4a-2) and TEM (Figure 4a-3) images in PBDThDTBT/PC$_{71}$BM blends. Some PC$_{71}$BM aggregated even ∼100 nm in size, which would diminish exciton migration to the donor/acceptor interface and is not favorable for charge separation.[47] When DIO was added, there was no obvious improvement about the phase separation, as shown in Figure 4b-2,b-3, and obvious PC$_{71}$BM aggregations can still be observed, which resulted in nearly no improvements about the J_{sc} and the FF dropped from 69.78% to 68.22%. As shown in Figure 4c-2,c-3, fibril-like polymer aggregations ∼25 nm in width were observed for PBDTchDTBT/PC$_{71}$BM blends without DIO.[48] However, typical exciton diffusion lengths for conjugated polymers are a few nanometers, and hence, the wider fibrils may affect the percentage of excitons that reach the

interface with the fullerene where charge generation occurs.[49] Therefore, relative low J_{sc} of 10.24 mA cm^{-2} and PCE of 5.7% were obtained for PBDTchDTBT/PC$_{71}$BM device without DIO. Interestingly, the fibril width was remarkably reduced to ∼7 nm (Figure 4d-2,d-3) after 3% DIO was added, and a nanoscale fibrillar network was observed, which is desired for better charge transfer according to Janssen's work,[50] and led to improvement of FF from 66.47% to 72.74%. The narrow fibril of the polymer is also beneficial for exciton diffusion to the PBDTchDTBT/PC$_{71}$BM interface then higher J_{sc} = 13.50 mA cm^{-2} was achieved.[50] Interestingly, the μ_{hole} of PBDThDTBT/PC$_{71}$BM declined from 3.08×10^{-5} cm^2 V^{-1} s^{-1} to 2.18×10^{-5} cm^2 V^{-1} s^{-1} when 1% DIO was added, however, the μ_{hole} of PBDTchDTBT/PC$_{71}$BM increased from 1.62×10^{-5} cm^2 V^{-1} s^{-1} to 3.46×10^{-5} cm^2 V^{-1} s^{-1} as 3% DIO was added (Figure S9). This regular pattern agreed with the morphology and phase separation changing in both the polymer/PC$_{71}$BM blends before and after DIO was added. Higher μ_{hole} is also beneficial for higher J_{sc} and FF.[51,52]

In conclusion, a reasonable conception of steric hindrance affecting D–A polymer's photophysical, electrochemical and photovoltaic characteristics is realized by a parallel comparison of hexyl and cyclohexyl substituted PBDTDTBTs. Our study indicates that the well designed steric hindrance can decrease both the HOMO and LUMO energy levels of the PBDT-DTBTs but cannot influence their E_g, which is very important for designing high efficiency OSC materials. Replacing hexyl by cyclohexyl results in higher V_{oc}, J_{sc}, and FF, and finally, highest PCE = 7.9% is realized in their OSCs devices.

■ ASSOCIATED CONTENT

Ⓢ Supporting Information

Experimental details on materials and methods, synthesis of monomers and polymers, thermal stability, hole mobility measurements, theoretical calculation, and device fabrication. This material is available free of charge via the Internet at http://pubs.acs.org.

■ AUTHOR INFORMATION

Corresponding Author

*E-mail: yangrq@qibebt.ac.cn.

Notes

The authors declare no competing financial interest.

■ ACKNOWLEDGMENTS

■ REFERENCES

(1) Burroughes, J. H.; Bradley, D. D. C.; Brown, A. R.; Marks, R. N.; Mackay, K.; Friend, R. H.; Burns, P. L.; Holmes, A. B. *Nature* **1990**, *347*, 539−541.

(2) Yu, G.; Gao, J.; Hummelen, J. C.; Wudl, F.; Heeger, A. J. *Science* **1995**, *270*, 1789−1790.

(3) Leclerc, M.; Morin, J. F. *Design and Synthesis of Conjugated Polymers*; John Wiley and Sons: New York, 2010.

(4) Günes, S.; Neugebauer, H.; Sariciftci, N. S. *Chem. Rev.* **2007**, *107*, 1324−1338.

(5) Thompson, B. C.; Fréchet, J. M. J. *Angew. Chem., Int. Ed.* **2008**, *47*, 58−77.

(6) Mei, J. G.; Bao, Z. N. *Chem. Mater.* **2013**, *26*, 604−615.

(7) Kline, R. J.; McGehee, M. D.; Kadnikova, E. N.; Liu, J. S.; Fréchet, J. M. J. *Adv. Mater.* **2003**, *15*, 1519−1522.

(8) Lei, T.; Wang, J. Y.; Pei, J. *Acc. Chem. Res.* **2014**, *47*, 1117−1126.

(9) Peet, J.; Heeger, A. J.; Bazan, G. C. *Acc. Chem. Res.* **2009**, *42*, 1700−1708.

(10) Andersson, M. R.; Berggren, M.; Inganäs, O.; Gustafsson, G.; Gustafsson-Carlberg, J. C.; Selse, D.; Hjertberg, T.; Wennerström, O. *Macromolecules* **1995**, *28*, 7525−7529.

(11) Cheng, Y. J.; Yang, S. H.; Hsu, C. S. *Chem. Rev.* **2009**, *109*, 5868−5923.

(12) Zhou, H. X.; Yang, L. Q.; You, W. *Macromolecules* **2012**, *45*, 607−632.

(13) Wang, Y. Y.; Heck, B.; Schiefer, D.; Agumba, J. O.; Sommer, M.; Wen, T.; Reiter, G. *ACS Macro Lett.* **2014**, *3*, 881−885.

(14) Melucci, M.; Favaretto, L.; Zanelli, A.; Cavallini, M.; Bongini, A.; Maccagnani, P.; Ostoja, P.; Derue, G.; Lazzaroni, R.; Barbarella, G. *Adv. Funct. Mater.* **2010**, *20*, 445−452.

(15) Ko, S. W.; Verploegen, E.; Hong, S. H.; Mondal, R.; Hoke, E. T.; Toney, M. F.; McGehee, M. D.; Bao, Z. N. *J. Am. Chem. Soc.* **2011**, *133*, 16722−16725.

(16) Berggren, M.; Inganäs, O.; Gustafsson, G.; Rasmusson, J.; Andersson, M. R.; Hjertberg, T.; Wennerström, O. *Nature* **1994**, *372*, 444−446.

(17) Berggren, M.; Gustafsson, G.; Inganäs, O.; Andersson, M. R.; Wennerström, O.; Hjertberg, T. *Adv. Mater.* **1994**, *6*, 488−490.

(18) Kraft, A.; Grimsdale, A. C.; Holmes, A. B. *Angew. Chem., Int. Ed.* **1998**, *37*, 402−428.

(19) Pei, J.; Yu, W. L.; Huang, W.; Heeger, A. *Acta Polym.* **1999**, *50*, 327−331.

(20) Pei, J.; Yu, W. L.; Huang, W.; Heeger, A. J. *Macromolecules* **2000**, *33*, 2462−2471.

(21) Heeger, A. J. *Adv. Mater.* **2014**, *26*, 10−28.

(22) Themans, B.; Salaneck, W. R.; Brédas, J. L. *Synth. Met.* **1989**, *28*, 359−364.

(23) Dennler, G.; Scharber, M. C.; Ameri, T.; Denk, P.; Forberich, K.; Waldauf, C.; Brabec, C. J. *Adv. Mater.* **2008**, *20*, 579−583.

(24) Ko, S. W.; Hoke, E. T.; Pandey, L.; Hong, S. H.; Mondal, R.; Risko, C.; Yi, Y. P.; Noriega, R.; McGehee, M. D.; Brédas, J. L.; Salleo, A.; Bao, Z. N. *J. Am. Chem. Soc.* **2012**, *134*, 5222−5232.

(25) Chen, C. P.; Hsu, H. L. *Macromol. Rapid Commun.* **2013**, *34*, 1623−1628.

(26) Liang, Y. Y.; Xu, Z.; Xia, J. B.; Tsai, S. T.; Wu, Y.; Li, G.; Ray, C.; Yu, L. P. *Adv. Mater.* **2010**, *22*, E135−E138.

(27) Zhou, H. X.; Yang, L. Q.; Stuart, A. C.; Price, S. C.; Liu, S. B.; You, W. *Angew. Chem., Int. Ed.* **2011**, *50*, 2995−2998.

(28) Lee, D. Y.; Hubijar, E.; Kalaw, G. J. D.; Ferraris, J. P. *Chem. Mater.* **2012**, *24*, 2534−2540.

(29) Nguyen, T. L.; Choi, H. S.; Ko, S. J.; Uddin, M. A.; Walker, B.; Yum, S. J.; Jeong, J. E.; Yun, M. H.; Shin, T. J.; Hwang, S. G. *Energy Environ. Sci.* **2014**, *7*, 3040−3051.

(30) Cui, C. H.; Wong, W. Y.; Li, Y. F. *Energy Environ. Sci.* **2014**, *7*, 2276−2284.

(31) Zhang, Y.; Chien, S. C.; Chen, K. S.; Yip, H. L.; Sun, Y.; Davies, J. A.; Chen, F. C.; Jen, A. K. Y. *Chem. Commun.* **2011**, *47*, 11026−11028.

(32) Lee, D. Y.; Stone, S. W.; Ferraris, J. P. *Chem. Commun.* **2011**, *47*, 10987−10989.

(33) Li, Z.; Lu, J. P.; Tse, S. C.; Zhou, J. Y.; Du, X. M.; Tao, Y.; Ding, J. F. *J. Mater. Chem.* **2011**, *21*, 3226−3233.

(34) Huang, Y.; Liu, F.; Guo, X.; Zhang, W.; Gu, Y.; Zhang, J. P.; Han, C. C.; Russell, T. P.; Hou, J. H. *Adv. Energy Mater.* **2013**, *3*, 930−937.

(35) Hou, Q.; Zhou, Q. M.; Zhang, Y.; Yang, W.; Yang, R. Q.; Cao, Y. *Macromolecules* **2004**, *37*, 6299−6305.

(36) Mei, C. Y.; Liang, L.; Zhao, F. G.; Wang, J. T.; Yu, L. F.; Li, Y. X.; Li, W. S. *Macromolecules* **2013**, *46*, 7920−7931.

(37) Frisch, M. J.; Trucks, G. W.; Schlegel, H. B.; Scuseria, G. E.; Robb, M. A.; Cheeseman, J. R.; Scalmani, G.; Barone, V.; Mennucci, B.; Petersson, G. A.; Nakatsuji, H.; Caricato, M.; Li, X.; Hratchian, H. P.; Izmaylov, A. F.; Bloino, J.; Zheng, G.; Sonnenberg, J. L.; Hada, M.; Ehara, M.; Toyota, K.; Fukuda, R.; Hasegawa, J.; Ishida, M.; Nakajima, T.; Honda, Y.; Kitao, O.; Nakai, H.; Vreven, T.; Montgomery, J. A.; Peralta, J. E.; Ogliaro, F.; Bearpark, M.; Heyd, J. J.; Brothers, E.; Kudin, K. N.; Staroverov, V. N.; Kobayashi, R.; Normand, J.; Raghavachari, K.; Rendell, A.; Burant, J. C.; Iyengar, S. S.; Tomasi, J.; Cossi, M.; Rega, N.; Millam, J. M.; Klene, M.; Knox, J. E.; Cross, J. B.; Bakken, V.; Adamo, C.; Jaramillo, J.; Gomperts, R.; Stratmann, R. E.; Yazyev, O.; Austin, A. J.; Cammi, R.; Pomelli, C.; Ochterski, J. W.; Martin, R. L.; Morokuma, K.; Zakrzewski, V. G.; Voth, G. A.; Salvador, P.; Dannenberg, J. J.; Dapprich, S.; Daniels, A. D.; Farkas, Ö.; Foresman, J. B.; Ortiz, J. V.; Cioslowski, J.; Fox, D. J. *Gaussian 09*, Revision A.1, Gaussian, Inc.: Wallingford, CT, 2009.

(38) Beaujuge, P. M.; Amb, C. M.; Reynolds, J. R. *Acc. Chem. Res.* **2010**, *43*, 1396−1407.

(39) Zhou, H. X.; Yang, L. Q.; Xiao, S. Q.; Liu, S. B.; You, W. *Macromolecules* **2009**, *43*, 811−820.

(40) Andersson, M. R.; Thomas, O.; Mammo, W.; Svensson, M.; Theander, M.; Inganäs, O. *J. Mater. Chem.* **1999**, *9*, 1933−1940.

(41) Wang, H. J.; Chou, C. W.; Chen, C. P.; Chen, Y. H.; Lee, R. H.; Jeng, R. J. *J. Mater. Chem. A* **2013**, *1*, 8950−8960.

(42) Zhou, H. X.; Yang, L. Q.; Stoneking, S.; You, W. *ACS Appl. Mater. Interfaces* **2010**, *2*, 1377−1383.

(43) Han, L. L.; Bao, X. C.; Hu, T.; Du, Z. K.; Chen, W. C.; Zhu, D. Q.; Liu, Q.; Sun, M. L.; Yang, R. Q. *Macromol. Rapid Commun.* **2014**, *35*, 1153−1157.

(44) Wang, N.; Chen, Z.; Wei, W.; Jiang, Z. H. *J. Am. Chem. Soc.* **2013**, *135*, 17060−17068.

(45) Peet, J.; Kim, J. Y.; Coates, N. E.; Ma, W. L.; Moses, D.; Heeger, A. J.; Bazan, G. C. *Nat. Mater.* **2007**, *6*, 497−500.

(46) Lee, J. K.; Ma, W. L.; Brabec, C. J.; Yuen, J.; Moon, J. S.; Kim, J. Y.; Lee, K. H.; Bazan, G. C.; Heeger, A. J. *J. Am. Chem. Soc.* **2008**, *130*, 3619−3623.

(47) Park, S. H.; Roy, A.; Beaupre, S.; Cho, S.; Coates, N.; Moon, J. S.; Moses, D.; Leclerc, M.; Lee, K. H.; Heeger, A. J. *Nat. Photonics* **2009**, *3*, 297−302.

(48) Li, W. W.; Hendriks, K. H.; Furlan, A.; Roelofs, W. S. C.; Meskers, S. C. J.; Wienk, M. M.; Janssen, R. A. J. *Adv. Mater.* **2014**, *26*, 1565−1570.

(49) Shaw, P. E.; Ruseckas, A.; Samuel, I. D. W. *Adv. Mater.* **2008**, *20*, 3516−3520.

(50) Li, W. W.; Hendriks, K. H.; Furlan, A.; Roelofs, W. S. C.; Wienk, M. M.; Janssen, R. A. J. *J. Am. Chem. Soc.* **2013**, *135*, 18942−18948.

(51) Price, S. C.; Stuart, A. C.; Yang, L. Q.; Zhou, H. X.; You, W. *J. Am. Chem. Soc.* **2011**, *133*, 4625−4631.

(52) Min, J.; Zhang, Z. G.; Zhang, S. Y.; Li, Y. F. *Chem. Mater.* **2012**, *24*, 3247−3254.